Woven Wire Gas-To-Liquid Heat Exchanger

Hannes Fugmann, Ahmed Junaid Tahir, Lena Schnabel
Fraunhofer ISE, Fraunhofer Institute for Solar Energy Systems
Heidenhofstr. 2, 79110 Freiburg, Germany
hannes.fugmann@ise.fraunhofer.de; ahmed.junaid.tahir@ise.fraunhofer.de;
lena.schnabel@ise.fraunhofer.de

Abstract -Gas-to-liquid heat exchangers lack in an adequate heat transfer coefficient on the gas side due to low convective heat transfer into the gas. Enhancing the heat transfer mechanism by increasing the surface area yields an improved heat transfer. Woven wire heat exchangers allow enlarging heat transfer surface area, decreasing material usage and the flexibility of different geometrical dimensions with the drawback of an increasing pressure drop. A further advantage of woven capillary-tube-and-wire structures is the possibility to combine the process of production of the mesh with contacting it to a tube. However studying heat transfer and hydraulics of woven capillary-tube-and-wire structures in experimental set-ups shows barriers in achieving good connection between wires and capillary tubes in first samplings. A medium heat transfer coefficient of 110 W/m²K for air velocities of 2 m/s with water as second fluid and stainless steel as solid structure can be achieved. Numerical simulations can reproduce the measurements and extended simulations of the same geometry, with less heat resistance between wires and tubes, yield a heat transfer coefficient of 330 W/m²K for a solid structure of 300 W/mK, showing the potential for wire structures as heat exchanger enhancer.

Keywords: wire structure; heat transfer; fluid dynamics; gas-to-liquid heat exchanger

1. Introduction

In general gas-to-liquid heat exchangers have a high heat transfer coefficient on the liquid side, but lack in good heat transfer characteristics on the gas side. This is represented by the low value of heat transfer coefficient from gases to surrounding heat transfer surfaces in a forced convection process. Thus an increase in efficiency of the heat exchanger can be achieved by concentrating on enhancements of the gas side heat transfer surface. The surface structure must fulfil four important aspects. Firstly the surface has to have a high surface area in comparison to the liquid side heat transfer surface area, secondly the enhancement should increase the heat transfer coefficient, while thirdly the pressure drop on the air side and fourthly the use of heat exchanger material should be as low as possible.

This enhancement is possible with structures having a low characteristic diameter and the flexibility of assembling it in a flow resistance minimizing way, whereas the heat conduction through the structure is optimal in orientation towards the primary surface. Wire mesh structures meet these requirements. They are widely used as filter media (Sun et al., 2015; Glatt et al., 2009) and as regenerators due to the high surface area density. For heat transfer enhancement in heat exchangers with low convective heat transport on the gas side a variety of different design ideas are shown in literature and on the market. Metallic woven wire mesh structures (Liu et al., 2015; Xu et al., 2007; Prasad et al., 2009) and screen-fin structures (Li, Wirtz, 2003) are contacted to a flat primary surface, separating the fluid from the heat source or sink. Whereas wire-on-tube type heat exchangers (Kumra et al., 2013; Lee et al., 2001) have to enable contact on rounded surfaces. Wire diameter ranges primarily from 100 µm to 1mm. In the literature named above the wire structure is woven or knitted separately from the process of contacting it to the primary surface. Combining the two surfaces, the primary surface and the surface enlargement with a wire structure, in one process is experimentally studied in (Vlot, 2003) and design ideas are patented in (Balzer, 2006; van Andel, van Andel, 2006). During this weaving process small capillary tubes are used

as weft instead of wire. In perpendicular direction wire in the order of 100 μm is used as warp. In this paper the thermodynamic behaviour of a woven capillary-tube-and-wire structure will be characterized by presenting experimental results on pressure drop and heat transfer and compared to simulation studies of fluid dynamics.

2. Woven Wire Heat Exchanger

Different geometrical configurations of wire structures are manufactured by the company Spörl KG (Web-1) for first tests of the production process and the measurement scope. One of the structures is shown in Fig. 1 (left). In this implementation the wire mesh width is very small, resulting in a tight textile. The geometrical possibilities can be realized by changing the wire diameter, the tube diameter and the distance of tube and wire in warp and weft direction.

Fig. 1. Left: Wire structure with mesh width of approximately 3 mm (warp direction) and 0.1 mm (weft direction). Right: CAD of woven wire heat exchanger with distributor/collector

The structures are made of stainless steel, the capillary tubes are diffusion welded to the wires and soldered to a distributor/collector. For thermodynamic characterization hot water is pumped through the distributor, the capillary tubes and the collector, while cold air flows perpendicular to the tubes through the structure and is heated up (see Fig. 1: right). The geometrical characteristics of one of the heat exchangers (HX1) with wire mesh structure are presented in Table 1.

Table. 1. Specification of woven wire heat exchanger geometry

Specification	Units	HX1
Number of capillary tubes	-	50
Outer / Inner diameter of capillary tubes	[mm]	2 / 1.9
Distance between centres of capillary tubes	[mm]	4.5
Length of capillary tubes	[mm]	205
Diameter of wires	[mm]	0.1
Number of wires	-	~ 740
Distance between centre of wires (on one side of capillary tube)	[mm]	0.5
Length of structure in wire direction	[mm]	231
Outer / Inner diameter of distributor and collector	[mm]	42 /38

In the first batch, weaving, welding and connecting the capillary tubes to the distributor and collector have yielded a displacement of the wires with respect to the tubes for structures with large mesh width. For the latest batch mesh width has been reduced, which will result in a higher pressure drop and a higher heat transfer, but yielded a more homogenous structure. The latest structure is shown in Fig. 2.

Fig. 2. Heat exchanger of the latest batch

3. Testing Facility and Simulation

3. 1. Testing Facility

For measuring pressure drop and heat transfer of gas flow through the heat exchanger a test rig has been installed at Fraunhofer ISE within the project Effimet (Web-2). Air and water can be used for characterizing gas-to-liquid heat exchangers. Prior to the test section containing the testing model (see Fig. 3), a flow conditioning section is installed on the air side. It comprises a chiller, an electric heater, a humidifier, a controllable fan and the respective sensors for air temperature, humidity and volume flow (nozzle). It can deliver temperatures in the range of 5 – 40 °C and volume flow rates between 150 – 1000 m³/h.
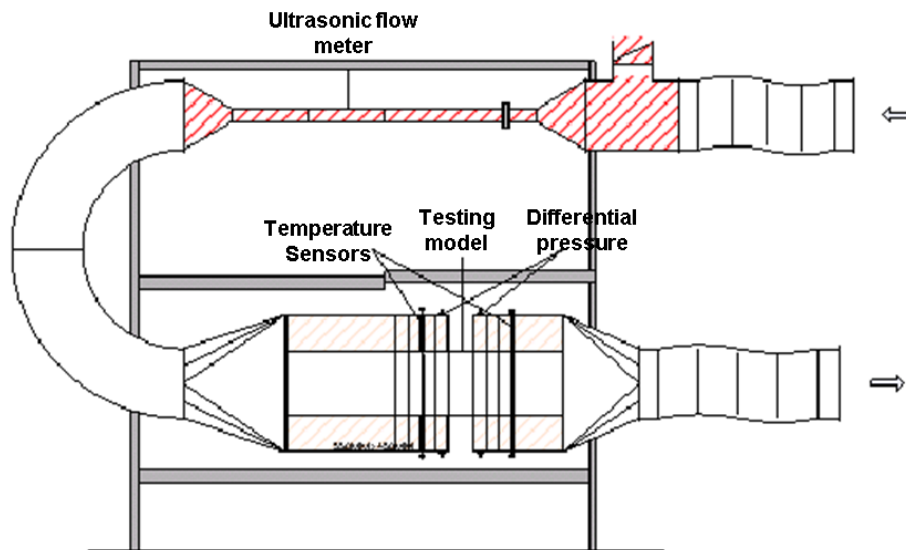
Fig. 3. Sketch of the air side of the heat exchanger test rig at Fraunhofer ISE; the air flow conditioning section is connected at the right side of the test rig.

In order to be able to measure heat exchangers at lower air volume flows a bypass valve is installed in the upper side of the test stand and a DN50 duct section with ultrasonic flow meter can be inserted into

the measurement channel. This way we can measure with air volume flows down to 10m³/h. Following the bend (DN280) is a 510 mm straight rectangular channel of 185 mm x 231 mm. In the test section fast reacting thin film Pt100 temperature sensors are used (Class A, uncertainty: 0.07 K). Four sensors are installed at the inlet channel, followed by two metal screens which ensure a uniform velocity profile. In the outlet channel 12 sensors record the temperature. All sensors are installed in the centre of squares of equal area. The pressure drop across the testing model is measured with two differential pressure transmitters (PU/PI, halstrup-walcher) with a measuring range of 0 – 50 Pa (for good accuracy at low pressure drops; uncertainty: 0.15 Pa) and 0 – 250 Pa (for higher pressure drops; uncertainty: 1.04 Pa). The entire testing section is leakage tested and thermally insulated.

On the water side temperature and volume flow rate can be controlled by a chiller/heater (Unichiller 017Tw-H, Huber) and measured with Pt100 resistance temperature sensors (Omnigrad T TST310, Endress+Hauser; uncertainty: 0.07 K) and an electromagnetic flow sensor (Optiflux 1000, Krohne). Pressure drop is measured via differential pressure transmitter (idm331, ICS Schneider Messtechnik GmbH).

During measurements the inlet air temperature is fixed to ambient temperature in order to avoid losses, while the water enters the heat exchanger at 60°C. The water flow rate is set to ~1 m³/h, therefore the change in water temperature across the heat exchanger is very small (<1K). For the characterization of heat exchangers the air volume flow is increased stepwise from 30m³/h to 800m³/h. The heat exchanged is then determined on the basis of the average air temperatures before and after the testing model.

3. 2. Simulation

As the wire structure is symmetric, simulating the flow can be reduced to a small segment of the heat exchanger, while later an upscaling is necessary to determine the performance of the whole heat exchanger. This segment is shown in Fig. 4 (left). It is given by two parts of the tube and the wired structure between the tubes. A heat transfer resistance between the outer wall of the tubes and the wire structure can be included to account for defective welding, either by inserting an air gap or a fixed volume with low conductivity between the wires and the tubes.
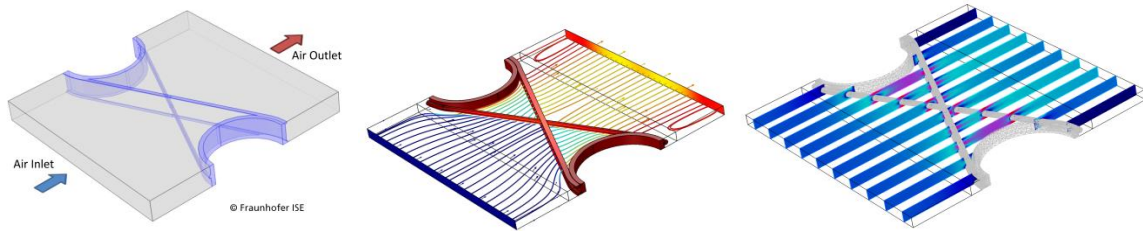
Fig. 4. Left: Simulated geometry showing the cold air entry and warm air exit. The wire structure and the tubes are shown in purple. Middle: Velocity streamlines and temperature distribution in air, in the tube wall and in the wire connecting the two tubes (red: warm; blue: cold). Right: Velocity magnitude in air (red: high; blue: low) and the meshing of the solid .

Fluid flow and heat transfer is simulated by using the finite element method (FEM), implemented in COMSOL Multiphysics® (Version 4.4). Boundary conditions for temperature, pressure and velocity are chosen to result in a steady state laminar flow. The simplified continuity equation, Navier Stokes Equation and energy equation are describing the system on the air side:

$$\nabla \cdot (\rho_{\text{air}} \, \mathbf{u}) = 0 \tag{1}$$

$$\rho_{\text{air}}(\mathbf{u} \cdot \nabla)\mathbf{u} = \nabla \cdot [\, -p\mathbf{I} + \mu_{\text{air}}(\nabla\mathbf{u} + (\nabla\mathbf{u})^{\text{T}}) - \tfrac{2}{3}\mu_{\text{air}}(\nabla \cdot \mathbf{u})\mathbf{I}] \tag{2}$$

$$\rho_{\text{air}} c_{p,\text{air}} \mathbf{u} \cdot \nabla T = \nabla \cdot (k_{\text{air}} \nabla T) \tag{3}$$

The energy (heat) equation describes the solid domain:

$$\nabla \cdot (k_{\text{solid}} \nabla T) = 0 \tag{4}$$

The material properties $\rho_{air}, \mu_{air}, c_{p,air}$ and k_{air} are the temperature and pressure dependent density, dynamic viscosity, heat capacity at constant pressure and thermal conductivity of air, while k_{solid} is the thermal conductivity of the wires and tubes and $\mathbf{I}$ is the identity. The scalars for temperature T and pressure p and the velocity field $\mathbf{u}$ are the dependent variables. The thermal conductivity of the solid k_{solid} is chosen to be 15 W/mK for comparison to the experiments (stainless steel) and increased up to 300 W/mK to express the potential for usage of high conductive materials as wires.

The water side is not simulated, as the mass flow on the water side in the experiment is so high, that the temperature experiences only a slight reduction. Instead a fixed temperature is set on the inner capillary tube wall as a boundary condition. Faces between solid and air domain are set to no-slip condition, at inlet resp. outlet faces velocity resp. pressure is fixed. All other boundaries are symmetric. The velocity streamlines, temperature distribution, velocity magnitude and the meshing of the solid for one of the geometries are depicted in Fig. 4.

3. 3. Comparison

For comparison to the experimental results the geometry of HX1 has been built in COMSOL Multiphysics® and simulation with different gap sizes between wire and capillary tube have been performed at different inlet velocities of air. Additionally the thermal conductivity of the capillary tubes and wires has been changed. Simulation and experimental results are presented in terms of a convective heat transfer coefficient and pressure drop, as well as in non-dimensional quantities.

The exchanger overall heat transfer rate equation is given by (cf. (Shah, R. K, Sekulić, 2003, p. 105)):

$$\dot{Q} = UA_{\text{HTS}}\Delta T_{\text{m}} \tag{5}$$

with the total heat transfer rate in an exchanger $\dot{Q}$, the overall heat transfer coefficient U, the heat transfer surface area A_{HTS} on the air side and the true (or effective) mean temperature difference (MTD), also referred to as mean temperature driving potential ΔT_m. In the simulation case the MTD equal the logarithmic temperature difference. For the experiment additional NTU-Method has been used to determine a correct MTD.

When a wire structure is contacted to tubes the same procedure can be applied to estimate the convective heat transfer coefficient as for classical fins. In this case we refer to a pseudo-convective heat transfer coefficient that includes the heat transfer from the air to the wire structure and the heat conduction through the solid towards the inner capillary tube wall (cf. (Hutter et al., 2011)). For the simulation this pseudo-convective heat transfer coefficient α equals U in Equation 5. For the experiments the heat resistance on the water side has to be eliminated from the overall heat transfer coefficient by

$$\frac{1}{\alpha} = \frac{1}{U} - \frac{A_{\text{HTS}}}{\alpha_{\text{water}} A_{\text{HTS,water}}} \tag{6}$$

to get the pseudo-convective heat transfer coefficient α. The heat transfer coefficient on the water side α_{water} has to be calculated based on available correlations in literature (cf. (Wärmeatlas, 2006)).

The Nusselt number Nu is a non-dimensional quantity, expressing the convective heat transfer versus the conductive heat transfer. It is defined as

$$\text{Nu} = \frac{\alpha d}{k_{\text{air}}} \tag{7}$$

Whereas d is a characteristic length of the wire heat exchanger ($d = 4A_0 L/A_{HTS}$ with minimum free flow area A_0 and length of heat exchanger in air flow direction L).

The pressure drop Δp is calculated by taking the difference of air inlet pressure and air outlet pressure. Its non-dimensional representative is the Fanning friction factor f which is given by

$$f = \frac{\Delta p}{4\left(\frac{L}{d}\right)\left(\frac{\rho_{\text{air}} u_{\text{air,inlet}}^2}{2\,\epsilon^2}\right)} \tag{8}$$

with $u_{\text{air,inlet}}$ representing the inlet velocity on the air side and ϵ being equal to the ratio of minimum free flow area A_0 and inlet cross flow area A_{in}. The non-dimensional quantities are correlated versus the Reynolds number

$$\text{Re} = \frac{\rho_{\text{air}} u_{\text{air,inlet}} d}{\mu_{air}\epsilon} \tag{9}$$

4. Results

The heat transfer of the woven wire heat exchanger (HX1) was much less than expected from simulations before. These first simulations did not include any additional heat resistance between the wires and the capillary tubes. As the HX1 is very inhomogeneous and some wires are not welded at all, a lower heat transfer is explainable. To quantify the heat resistance, an additional gap between the wires and the capillary tubes was added in the simulation. An air gap of 0.02mm is found to fit the measurement data best. In Fig. 5 the pseudo-convective heat transfer coefficient α is plotted versus air inlet velocity $u_{\text{air,inlet}}$ for simulations and measurements with two thermal conductivities of the wires and capillary tubes of k_{solid} = 15 W/mK and k_{solid} = 300 W/mK. The later conductivity shall express a potential for wire structures with highly conductive material instead of stainless steel. Results with and without a heat resistance between the wire and the capillary tubes, expressed by a gap between the two of 0.02 mm are shown as well.

The potential for a highly conductive material used as solid (with the same design as used in this study) is very high, yielding pseudo-convective heat transfer coefficients of more than 400 W/m²K for velocities of 3 m/s. Classical extended surfaces (wavy, offset strip, louvered, etc.) achieve coefficients in the range of 50 W/m²K (cf. (Hesselgreaves, 2001)). The volume specific heat transfer surface area in the simulation model is 990 m²/m³ and therefore belonging to the class of compact heat exchangers (cf. definition in (Shah, R. K, Sekulić, 2003): surface area density greater than about 700 m²/m³). Therefore the product of both pseudo-convective heat transfer coefficient and heat transfer surface area in relation to the total volume is very high. Likewise heat transfer surface area is high in comparison to the used material volume of wires and capillary tubes with a value of more than 15000 m²/m³.

A high consistency of pressure drop measurement and simulation is given for all three presented simulations, as the change in geometry is marginal and the change in solid thermal conductivity does influence the flow only by a change in fluid temperature and therefore in the fluid properties ρ_{air} and μ_{air} (see Fig. 6). Relative errors are maximum 8% and therefore out of the range of the measurement error for pressure drop (0.15 Pa). An explanation for this (slight) error can be that fluid dynamics differs due to the inhomogeneous wire structure in comparison to the symmetric simulation model. In comparison to standard heat transfer enhancers, such as offset strip fins, the pressure drop is slightly higher for equal fluid flow length.
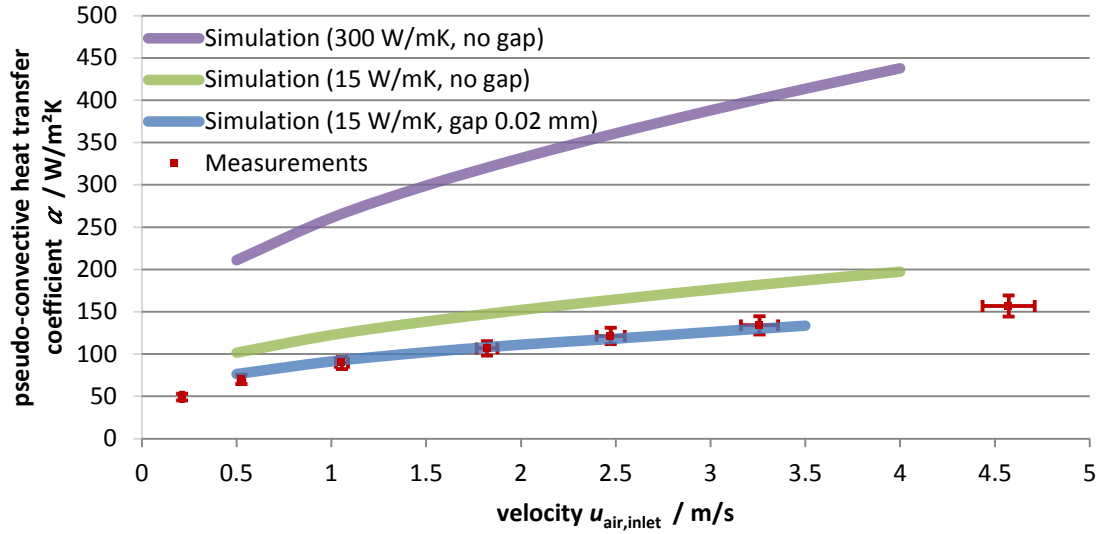
Fig. 5. Pseudo-convective heat transfer coefficient α versus air inlet velocity $u_{air,inlet}$ for simulations and measurements with different thermal conductivities of the wires and capillary tubes and for different heat resistance between the wire and the capillary tubes.
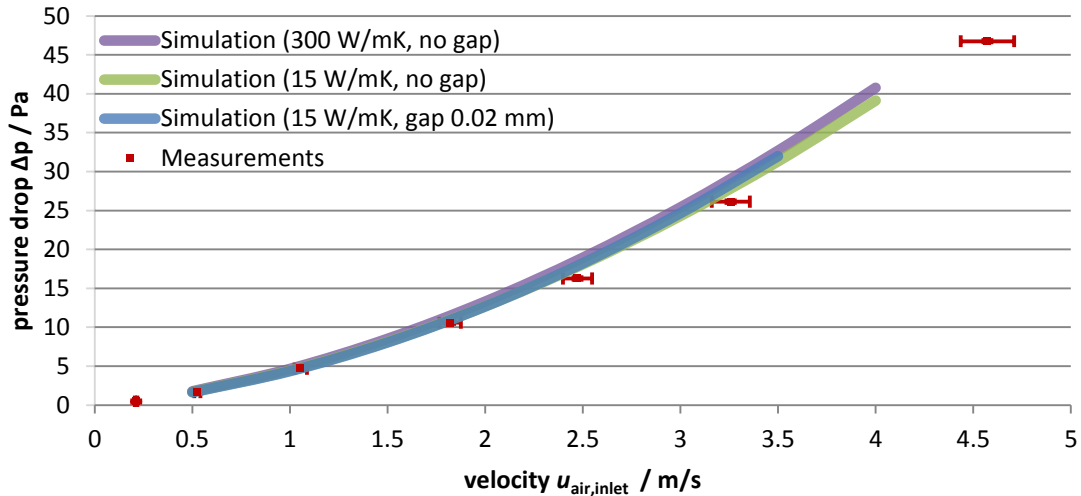
Fig. 6. Pressure drop Δp versus air inlet velocity $u_{air,inlet}$ for simulations and measurements.

The Fanning friction factor and Nusselt number of the measurement data is correlated via the following equations to the Reynolds number (by means of minimizing least square error of data):

$$f = 4.10\,\mathrm{Re}^{-0.50} \tag{10}$$

$$\mathrm{Nu} = 0.78\mathrm{Re}^{0.37} \tag{11}$$

Reynolds numbers range from 50 to 1150 for air velocities at the inlet of 0.2 m/s to 4.5 m/s.

5. Conclusion

Woven wire structures allow heat exchanger design with a noticeable geometrical flexibility, potentially high heat transfer coefficients (in this numerical study: 400 W/m²K at 3 m/s) and high specific heat transfer surface area with respect to total heat exchanger volume or material volume for wires and capillary tubes. Pressure drop characteristics can be met by simulations with relative errors below 8%, while heat transfer can only be simulated with good agreement to the measurement data by adding a heat resistance between wires and capillary tubes and fitting the describing parameter to the measured data. The calculated potential in heat transfer based on simulations for this non-optimized design is approximately three times higher than the measured heat transfer characteristics, presuming an even higher potential for a geometrically optimized structure.

Future work will focus on an optimized process of contacting wires and capillary tubes, on the use of highly conductive wire materials and on a suitable assembly of multiple structures in succession.

Acknowledgements

References

Balzer, R. (2006). Wärmetauschvorrichtung für einen Wärmeaustausch zwischen Medien und Webstruktur. *Patent no. DE102006022629 A1.*

Glatt, E., Rief, S., Wiegmann, A., Knefel, M., & Wegenke, E., (2009). Structure And Pressure Drop Of Real And Virtual Metal Wire Meshes. *Edited by ITWM.*

Hesselgreaves, J., (2001). Compact Heat Exchangers. *Selection, Design, And Operation.* Amsterdam, New York: Pergamon.

Hutter, C., Büchi, D., Zuber, V., & Rudolf von Rohr, Ph. (2011). Heat Transfer In Metal Foams And Designed Porous Media. *Chemical Engineering Science,* 66(17), 3806–3814. DOI:10.1016/j.ces.2011.05.005.

Kumra, A., Rawal, N., & Samui, P., (2013). Prediction of Heat Transfer Rate of a Wire-on-Tube Type Heat Exchanger: An Artificial Intelligence Approach. *Procedia Engineering,* 64, 74–83. DOI:10.1016/j.proeng.2013.09.078.

Lee, T.H., Yun, J.-Y., Lee, J.-S., Park, J.-J., & Lee, K.-S. (2001). Determination Of Airside Heat Transfer Coefficient On Wire-On-Tube Type Heat Exchanger. *International Journal of Heat and Mass Transfer,* 44(9), 1767–1776.

Li, C., & Wirtz, R., (Eds.) (2003). Development Of A High Performance Heat Sink Based On Screen-Fin Technology. *IEEE.*

Liu, Y., Xu, G., Luo, X., Li, H., & Ma, J. (2015). An Experimental Investigation On Fluid Flow And Heat Transfer Characteristics Of Sintered Woven Wire Mesh Structures. *Applied Thermal Engineering,* 80, 118–126. DOI:10.1016/j.applthermaleng.2015.01.050.

Prasad, S. B., Saini, J. S., & Singh, K. M. (2009). Investigation Of Heat Transfer And Friction Characteristics Of Packed Bed Solar Air Heater Using Wire Mesh As Packing Material. *Solar Energy,* 83(5), 773–783. DOI:10.1016/j.solener.2008.11.011.

Shah, R. K., & Sekulić, D. P. (2003). Fundamentals Of Heat Exchanger Design. Hoboken (N.J.): Wiley.

Sun, H., Bu, S., & Luan, Y. (2015). A High-Precision Method For Calculating The Pressure Drop Across Wire Mesh Filters. *Chemical Engineering Science,* 127, 143–150. DOI:10.1016/j.ces.2015.01.023.

van Andel, E., & van Andel, E., (2006). Heat Exchanger And Applications Thereof. Patent no. US7963067 B2.

Vlot, M.B.A. (2003). Experimental Study on the Friction and Heat Transfer in a Fiwihex. *Master thesis.* Delft University of Technology, Delft. Kramers Laboratorium voor Fysische Technologie.

Wärmeatlas (2006). Verein Deutscher Ingenieure, VDI. *Springer Verlag, Berlin, Heidelberg, New York* (2).

Xu, J., Tian, J., Lu, T. J., & Hodson, H. P. (2007). On The Thermal Performance Of Wire-Screen Meshes As Heat Exchanger Material. *International Journal Of Heat And Mass Transfer,* 50(5-6), 1141–1154. DOI:10.1016/j.ijheatmasstransfer.2006.05.044.

Web sites:
Web-1: http://www.spoerl.de/, consulted 30 March 2015.
Web-2: http://effimet.com/, consulted 30 March 2015.
Web-3: https://www.solarueck.de/, consulted 30 March 2015.